European Journal of Radiology 181 (2024) 111728

Contents lists available at ScienceDirect

European Journal of Radiology

journal homepage: www.elsevier.com/locate/ejrad

Research article

Intra-individual comparison of epicardial adipose tissue characteristics on coronary CT angiography between photon-counting detector and energy-integrating detector CT systems

Dmitrij Kravchenko [a,b,c], Milan Vecsey-Nagy [a,d], Giuseppe Tremamunno [a,e], U. Joseph Schoepf [a], Jim O'Doherty [a,f], Julian A. Luetkens [b,c], Daniel Kuetting [b,c], Alexander Isaak [b,c], Muhammad Taha Hagar [a,g], Tilman Emrich [a,h,i,*], Akos Varga-Szemes [a]

[a] Division of Cardiovascular Imaging, Department of Radiology and Radiological Science, Medical University of South Carolina, Charleston, USA
[b] Department of Diagnostic and Interventional Radiology, University Hospital Bonn, Bonn, Germany
[c] Quantitative Imaging Laboratory Bonn (QILaB), Bonn, Germany
[d] Heart and Vascular Center, Semmelweis University, Budapest, Hungary
[e] Department of Medical Surgical Sciences and Translational Medicine, Sapienza University of Rome – Radiology Unit – Sant'Andrea University Hospital, Via di Grottarossa, 1035-1039, 00189, Rome, Italy
[f] Siemens Medical Solutions USA Inc, Malvern, USA
[g] Department of Diagnostic and Interventional Radiology, Medical Center, Faculty of Medicine, University of Freiburg, Hugstetter Straße 55, Freiburg im Breisgau 79106, Germany
[h] Department of Diagnostic and Interventional Radiology, University Medical Center of the Johannes Gutenberg-University, Mainz, Germany
[i] German Centre for Cardiovascular Research, Partner site Rhine-Main, Mainz, Germany

ARTICLE INFO

Keywords:
Epicardial adipose tissue
Photon-counting detector CT
Energy-integrating detector CT

ABSTRACT

Purpose: To explore the potential differences in epicardial adipose tissue (EAT) volume and attenuation measurements between photon-counting detector (PCD) and energy-integrating detector (EID)-CT systems.
Methods: Fifty patients (mean age 69 ± 8 years, 41 male [82 %]) were prospectively enrolled for a research coronary CT angiography (CCTA) on a PCD-CT within 30 days after clinical EID-based CCTA. EID-CT acquisitions were reconstructed using a Bv40 kernel at 0.6 mm slice thickness. The PCD-CT acquisition was reconstructed at a down-sampled resolution (0.6 mm, Bv40; [PCD-DS]) and at ultra-high resolutions (PCD-UHR) with a 0.2 mm slice thickness and Bv40, Bv48, and Bv64 kernels. EAT segmentation was performed semi-automatically at about 1 cm intervals and interpolated to cover the whole epicardium within a threshold of −190 to −30 HU. A subgroup analysis was performed based on quartile groups created from EID-CT data and PCD-UHR$_{Bv48}$ data. Differences were measured using repeated-measures ANOVA and the Friedman test. Correlations were tested using Pearson's and Spearman's rho, and agreement using Bland-Altman plots.
Results: EAT volumes significantly differed between some reconstructions (e.g. EID-CT: 138 ml [IQR 100, 188]; PCD-DS: 147 ml [110, 206]; P<0.001). Overall, correlations between PCD-UHR and EID-CT EAT volumes were excellent, e.g. PCD-UHR$_{Bv48}$: r: 0.976 (95 % CI: 0.958, 0.987); P<0.001; with good agreement (mean bias: −9.5 ml; limits of agreement [LoA]: −40.6, 21.6). On the other hand, correlations regarding EAT attenuation was moderate, e.g. PCD-UHR$_{BV48}$: r: 0.655 (95 % CI: 0.461, 0.790); P<0.001; mean bias: 6.5 HU; LoA: −2.0, 15.0.
Conclusion: EAT attenuation and volume measurements demonstrated different absolute values between PCD-UHR, PCD-DS as well as EID-CT reconstructions, but showed similar tendencies on an intra-individual level. New protocols and threshold ranges need to be developed to allow comparison between PCD-CT and EID-CT data.

Abbreviations: ADMIRE, Advanced Modeled Iterative Reconstruction; CACS, Coronary artery calcium score; CAD, coronary artery disease; CAD-RADS, Coronary artery disease reporting and data system; CCTA, Coronary computed tomography angiography; DS, Down-sampled; EAT, Epicardial adipose tissue; EID, Energy-integrating detector; MACE, Major adverse cardiac events; PCD, Photon-counting detector; QIR, Quantum iterative reconstruction; UHR, Ultra-high resolution.

* Corresponding author at: University Medical Centre of the Johannes Gutenberg University Mainz, Universitatsmedizin der Johannes Gutenberg-Universitat Mainz, Mainz 55131, Germany.
E-mail address: tilman.emrich@unimedizin-mainz.de (T. Emrich).

https://doi.org/10.1016/j.ejrad.2024.111728
Received 27 August 2024; Accepted 4 September 2024
Available online 7 September 2024

1. Introduction

Abnormalities in epicardial adipose tissue (EAT), defined as metabolically active fat between the myocardium and the visceral layer of the pericardium, have been shown to be associated with cardiovascular disease including coronary artery disease (CAD) [1,2]. It is believed that inflammation substantially contributes to the formation of atherosclerotic plaques and that adipose tissue is a significant source of proinflammatory mediators [3]. According to current guidelines, coronary CT angiography (CCTA) is the modality of choice for the assessment of CAD, allowing an alternative to invasive coronary angiography [4,5]. With the introduction of photon-counting detector CTs (PCD-CTs), CCTA was further improved with more accurate luminal stenosis grading thanks to an increased spatial resolution and always-on spectral imaging compared to energy-integrating detector CTs (EID-CTs) [6]. In addition to EAT volume being linked to inflammation and CAD, EAT density seems also to play a pivotal role, as lower densities of EAT have been correlated with major adverse cardiac events (MACE) [6–8]. However, EAT volume as well as attenuation are affected by acquisition and reconstruction parameters such as kernel selection, slice thickness, and tube voltage [9]. Currently, there is a paucity of data available regarding EAT volume and attenuation measurements on PCD-CTs.

Therefore, the aim of this study was to explore the potential differences in EAT volume and attenuation measurements between PCD and EID-CT systems on an intra-individual level.

2. Materials and Methods

2.1. Ethics and study population

This HIPAA compliant single-center study received approval from the local Institutional Review Board. Participants provided written informed consent before enrollment. Prospectively enrolled, consecutive patients who underwent clinically indicated CCTA on an EID-CT system between April 2023 and January 2024, and a research PCD-CT CCTA within 30 days of the initial scan were considered for inclusion in the study (Fig. 1). Inclusion criteria comprised patients aged 18 years and above undergoing standard CCTA on EID-CT for stable chest pain or planning for transcatheter aortic valve replacement. Exclusion criteria included contraindications to iodinated contrast media, decreased renal function (glomerular filtration rate < 45 ml/min/m^2), absence of coronary calcification on EID-CT, pregnancy or breastfeeding, inability to provide consent, or artefacts affecting segmentation.

2.2. CT acquisitions and reconstructions

All patients underwent electrocardiogram gated CCTA. EID-CT scans were performed on a third-generation dual-source EID-CT system (SOMATOM Force, Siemens Healthineers, Forchheim, Germany) using a standard of care protocol with automated exposure control (CARE-Dose4D, Siemens) and the following parameters: collimation, 192 $\times$ 0.6 mm, tube potential ranging from 90 to 130 kVp, and tube current–time product from 150 to 600 mAs. Patients with stable angina and a heart rate of less than 80 beats per minute were examined between the 30–90 % R-R interval after the administration of sublingual nitroglycerin (0.4 mg). All other patients were scanned using a retrospectively gated electrocardiogram protocol. All patients received a non-contrast scan on the EID-CT for calcium scoring and contrast enhanced CCTA after intravenous iodinated contrast media injected at 3.5–4.5 ml/s (weight dependent, 56–70 ml of iohexol [Omnipaque 350, GE Healthcare] or iopromid [Ultravist 370, Bayer Healthcare]).

PCD-CCTAs were acquired using a dual-source CT system (NAEOTOM Alpha, software version VA50, Siemens Healthineers) at 120 kVp and a collimation of 120 $\times$ 0.2 mm. Due to the research nature of the PCD-CT examination, no non-contrast datasets were acquired. The same acquisition mode and intravenous contrast injection protocol was used on the PCD-CT research scan as on the initial EID-CT examination.

Images were reconstructed using a proprietary offline software solution (ReconCT, version 17.1.0.644, Siemens Healthineers). EID-CT acquisitions were reconstructed with a slice thickness/increment of 0.6/0.4 mm, Advanced Modeled Iterative Reconstruction (ADMIRE) level 3, and a smooth, edge enhancing body/vascular kernel (Bv40). To best approximate an EID-CT reconstruction, a down-sampled PCD-CT reconstruction using a slice thickness/increment of 0.6/0.4 mm [PCD-DS] was performed using a matched kernel (Bv40). Furthermore, ultra-high resolution (UHR) PCD-CT reconstructions with a slice thickness/increment of 0.2/0.2 mm and Bv40, Bv48, and Bv64 kernels were reconstructed. Quantum iterative reconstruction (QIR) was set to level 4. All reconstructions were analyzed using dedicated software (Syngo.via, version VB70, Siemens Healthineers).

2.3. Epicardial adipose tissue measurements

A board-certified radiologist with 6 years of experience in cardiovascular imaging (D.Kr.) blinded to the patient's medical history quantified EAT on CCTA scans semi-automatically using a dedicated prototype software (Syngo.via Frontier, CT Cardiac Risk Assessment,

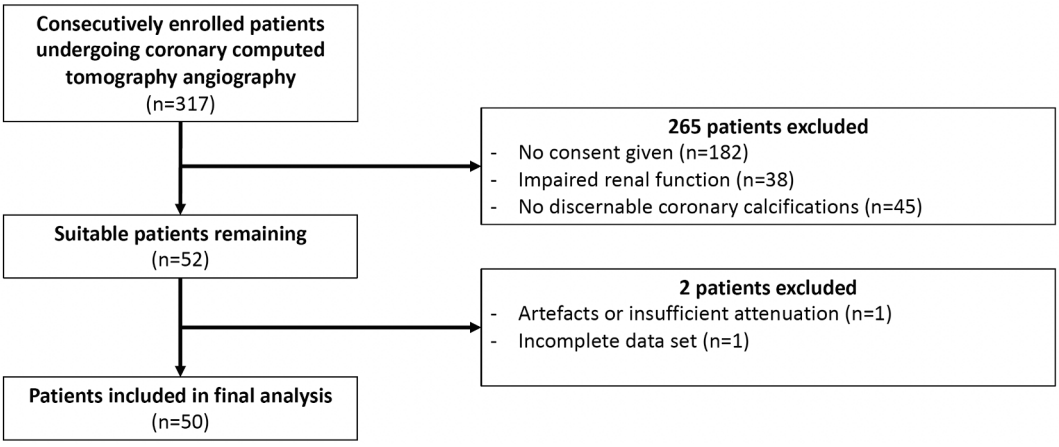

Fig. 1. Flowchart depicting patient recruitment.

Siemens Healthineers). EAT was defined as tissue with attenuation between −190 and −30 HU contained between the epicardium and pericardium [10]. Regions of interest were manually defined by tracing the pericardium on axial images from the pulmonary trunk to the apex of the heart at about 1 cm intervals, using a previously described technique [11]. Automatic software interpolation was then used to create a 3-dimensional volume of interest around the heart. For all PCD-CT reconstructions, a single segmentation was performed on PCD-CT$_{Bv48}$ images and a mask exported. The mask was then applied to all other PCD-CT reconstructions and checked for fit. A coronary artery disease reporting and data system (CAD-RADS) score was calculated. The Agatston score was used to calculate the coronary artery calcium score (CACS). The patient cohort was then split into quartiles based on EAT volume on the EID-CT and PCD-CT (kernel with the closest matching attenuation histogram to the EID-CT) for further subgroup analyses.

2.4. Statistical assessment

Statistical analyses were performed using commercially available statistics software (Prism [version 9.5.1; GraphPad Software] and SPSS [version 29.0; IBM SPSS statistics]). The Shapiro-Wilk test was used to assess data for normal distribution. Continuous data are expressed as mean and standard deviation or as median and interquartile range when a normal distribution could not be assumed. Ordinal data are presented as frequency. Repeated measures analysis of variance (RM-ANOVA) was used to compare means of three or more groups for data with normal distribution with Tukey's post hoc test. The Friedman test with Dunn's multiple comparison test was used to compare three or more groups when normality could not be assumed. Pearson's correlation was used for parametric data while Spearman's correlation was used for nonparametric data. The Phi coefficient was used to test for association between dichotomous and continuous data. The Kruskal-Wallis test was used to compare nonparametric data of more than two groups with Dunnett's T3 post hoc test. The Kruskal-Wallis H test or the Wilcoxon matched sign rank test was used to compare ordinal data. A P-value of < 0.05 was considered statistically significant.

3. Results

3.1. Epicardial adipose tissue volume and attenuation

Patient characteristics are found in Table 1. Multiple comparisons between EAT volume and attenuation on differing reconstructions are summarized in Table 2 and Fig. 2. An exemplary side-by-side comparison of EAT segmentation and attenuation curves for each reconstruction is presented in Fig. 3.

Table 1
Patient characteristics and coronary computed tomography angiography results.

	EID-CT	PCD-CT	P value
Age (years)		69 ± 8	
Sex (males n, %)		41 (82 %)	
Body mass index (kg/m^2)		31 ± 5	
Cardiovascular risk factors			
Hypertension (n, %)		34 (68 %)	
Diabetes (n, %)		10 (20 %)	
Family history for cardiovascular disease (n, %)		12 (24 %)	
Hyperlipidemia (n, %)		34 (68 %)	
Currently smoking (n, %)		2 (4 %)	
Coronary artery calcium score*		442 (159–969)	
Heart rate (bpm)	69 ± 10	67 ± 11	0.171
CAD-RADS	3.6 ± 0.7	3.1 ± 0.9	<0.001
Lowest FFR-score	0.55 ± 0.23	0.58 ± 0.24	0.091
Total coronary calcium volume (mm^3)*	342 (180, 608)	344(174, 606)	0.505
Total coronary plaque volume (mm^3)*	1085(711, 1610)	724(501, 1185)	<0.001

All values are given as means with standard deviation unless otherwise noted.
EID-CT: Energy-integrating detector CT. PCD: Photon-counting detector. DS: Downsampled to 0.6 mm. bpm: Beats per minute. CAD-RADS: Coronary artery disease reporting and data system. FFR: Fractional flow reserve.
* median and interquartile range.

Table 2
Comparison of epicardial adipose tissue measurements between all reconstructions.

Parameters	EID-CT	PCD-DS	PCD-UHR$_{Bv40}$	PCD-UHR$_{Bv48}$	PCD-UHR$_{Bv64}$	P value
EAT volume (ml)*	138 (100, 188)	147 (110, 206)	144 (108, 197)	146 (112, 193)	148 (108, 199)	<0.001
Dunn's multiple comparisons test P values for EAT volume						
EID-CT		**<0.001**	0.065	**<0.001**	**<0.001**	
PCD-DS			**<0.001**	**0.024**	0.054	
PCD-Bv40				0.877	0.500	
PCD-Bv48					0.999	
EAT attenuation (HU)	−78 ± 6	−80 ± 6	−81 ± 5	−84 ± 5	−91 ± 4	<0.001
Tukey's multiple comparisons test P values for EAT attenuation						
EID-CT		**0.019**	**<0.001**	**<0.001**	**<0.001**	
PCD-DS			0.500	**<0.001**	**<0.001**	
PCD-Bv40				**<0.001**	**<0.001**	
PCD-Bv48					**<0.001**	

All values are given as means with standard deviation unless otherwise noted.
EAT: Epicardial adipose tissue. EID-CT: Energy-integrating detector CT. PCD: Photon-counting detector. DS: Down-sampled to 0.6 mm. UHR: Ultra-high resolution. Bv: Body/Vascular kernels. HU: Hounsfield units.
* median and interquartile range.

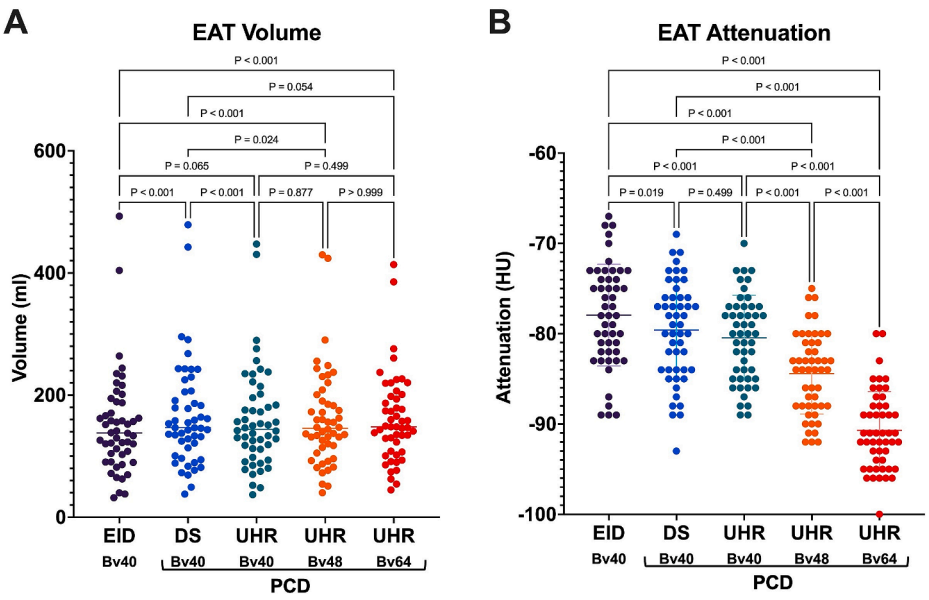

Fig. 2. Scatter plots comparing the median volume (A) of the epicardial adipose tissue (EAT) and the mean of the attenuation measured in Hounsfield units (HU) (B). Comparisons were performed on the same patients scanned on an energy-integrating detector CT (EID) and a photon-counting detector CT (PCD). PCD-CT reconstructions were down-sampled to match the resolution (0.6 mm) and kernel of the EID system (PCD-DS), with further reconstructions using ultra-high resolution (UHR) 0.2 mm slice thickness and different levels of kernel sharpness.

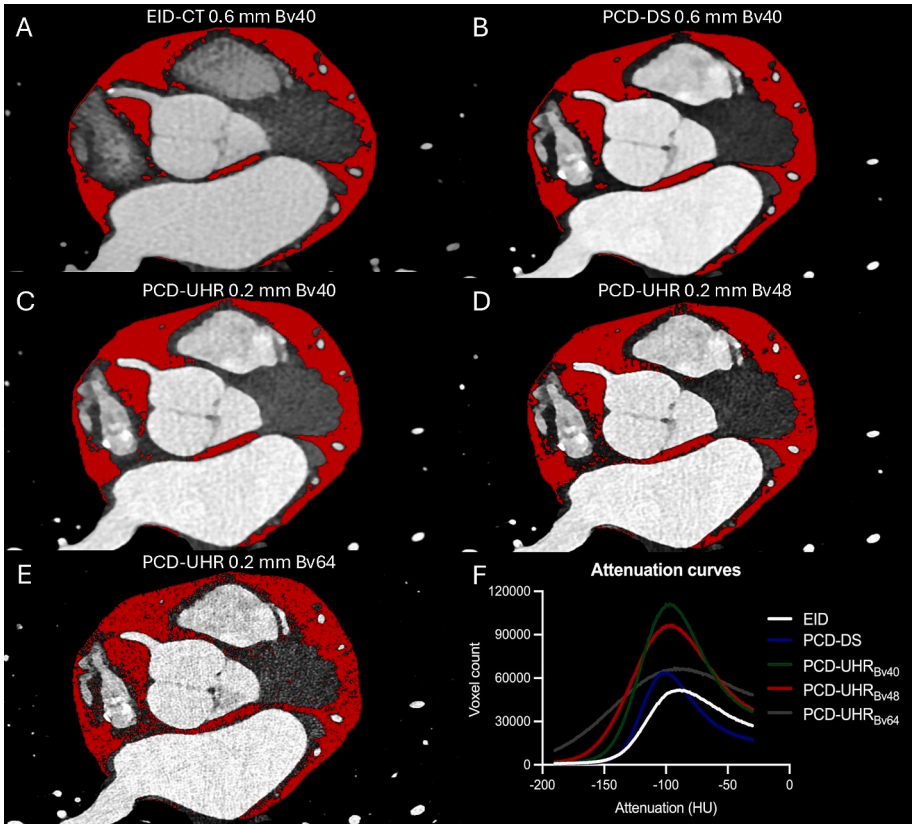

Fig. 3. Axial images of the heart at the origin of the right coronary artery of the same patient scanned on an energy-integrating detector CT (EID-CT) (A) and different reconstructions of a photon-counting detector CT (PCD-CT) acquisition. PCD-CT reconstructions included a down-sampled (PCD-DS) reconstruction to match the EID-CT (B) and variations in convolution kernel sharpness (C-E) of ultra-high resolution (UHR) reconstructions. Attenuation curves of the respective reconstructions demonstrating voxels between −190 and −30 HU (F).

3.2. Correlations

Spearman's correlation revealed very strong correlations between all volume measurements while Pearson's correlation demonstrated a moderate relationship between attenuations. Bland-Altman plots demonstrated good agreement between all volume and attenuation measurements (Figs. 4 and 5, details are given in Table A.1 of the Appendix). Correlations between EAT volume and age, heart rate, CACS,

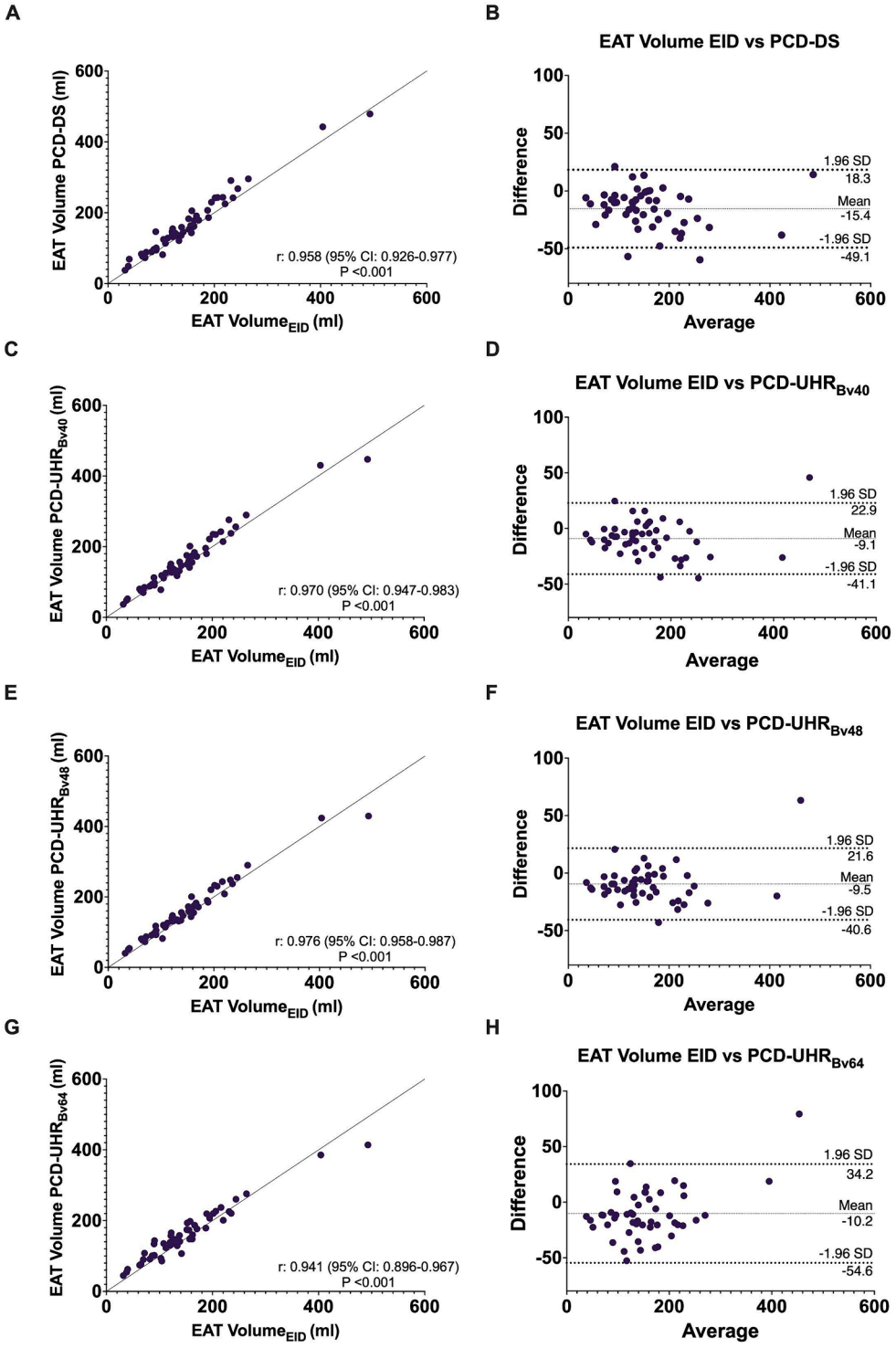

Fig. 4. Spearman's correlation (A,C,E,G) and Bland-Altman plots (B,D,F,H) comparing epicardial adipose tissue (EAT) volume measurements between energy-integrating detector CT (EID-CT) and variations in the photon-counting detector (PCD) CT reconstructions using a down-sampled slice thickness of 0.6 mm (PCD-DS) and ultra-high resolutions (PCD-UHR) with a 0.2 mm slice thickness and different kernels.

CAD-RADS, and total coronary calcium volume and total plaque volume were noted while inverse correlations between EAT attenuation and hyperlipidemia, current smoking status, CACS, CAD-RADS, and total coronary calcium volume and total plaque volume were also observed for the EID-CT. Patient parameters were further correlated to the PCD reconstruction most similarly matching the EID-CT. Detailed findings are given in Table 3.

3.3. Subgroup analysis

The cohort was split into quartiles of EAT volume based on measurements performed on the EID-CT system (group 1: < 99.7 ml, group 2: 99.8 to 138.1 ml, group 3: 138.2 to 187.8 ml, and group 4: >187.9 ml), and on PCD-CT EAT volume measurement on the Bv48 reconstruction (group 1: < 112.0 ml, group 2: 112.1 to 145.6 ml, group 3: 145.7 to 192.8 ml, and group 4: >192.9 ml). The results are provided in

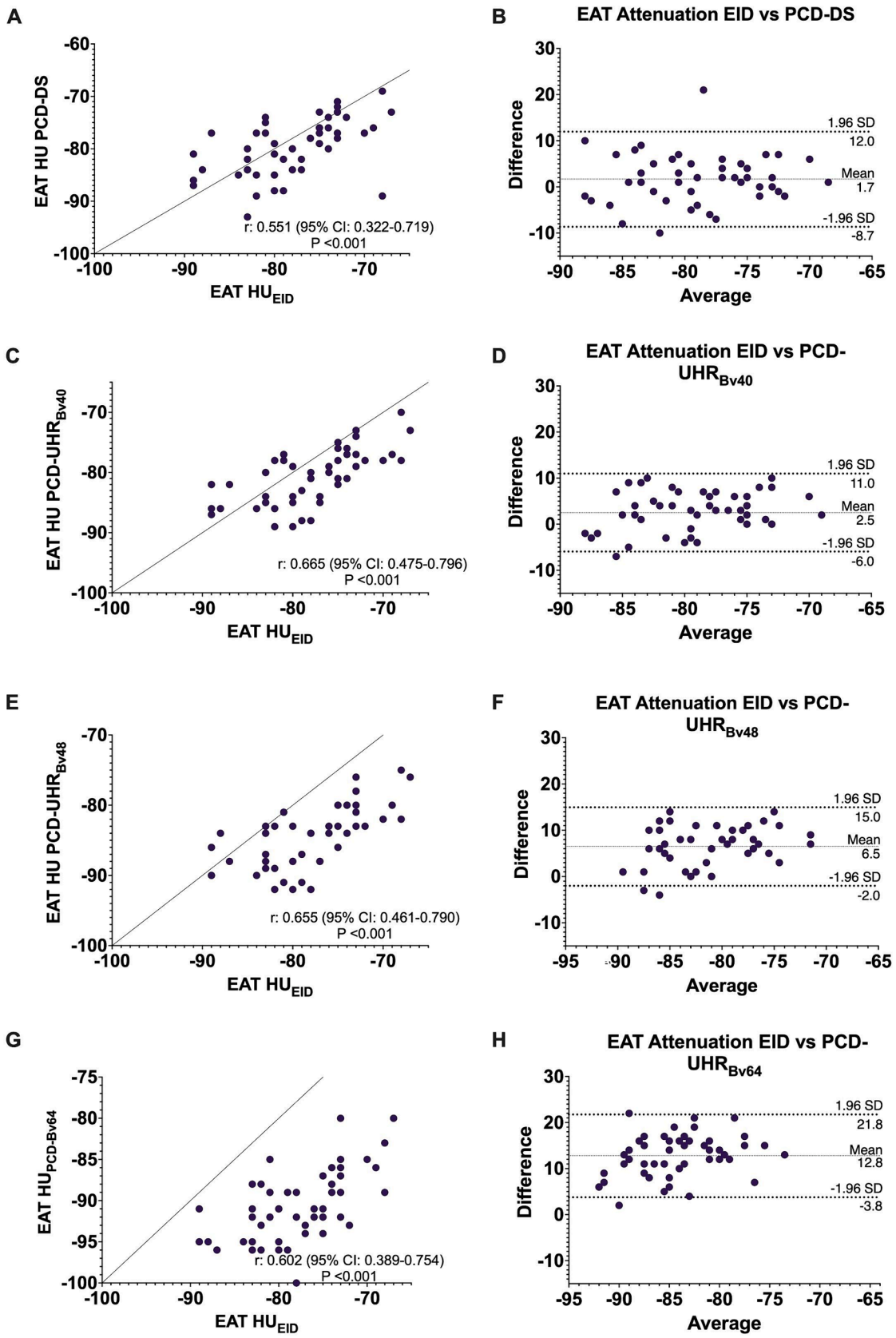

Fig. 5. Pearson's correlation (A,C,E,G) and Bland-Altman plots (B,D,F,H) comparing epicardial adipose tissue (EAT) attenuation measurements between the energy-integrating detector CT (EID-CT) and variations in the photon-counting detector (PCD) CT reconstructions using a down-sampled slice thickness of 0.6 mm (PCD-DS) and at ultra-high resolutions (PCD-UHR) with a 0.2 mm slice thickness and different kernels.

Table 3
Spearman's and Pearson's correlations for epicardial adipose tissue volume and attenuation on energy-integrating and photon-counting detector CT.

	EID				**PCD-UHR$_{Bv48}$**			
	EAT volume*		EAT attenuation		EAT volume*		EAT attenuation	
Parameter	r	95 % CI	r	95 % CI	r	95 % CI	r	95 % CI
Age (years)	**0.417**	0.149, 0.629	−0.111	−0.377, 0.173	**0.415**	0.146, 0.627	0.017	−0.262, 0.294
Sex (female)	−0.204	−0.463, 0.087	0.079	−0.204, 0.350	−0.171	−0.436, 0.121	−0.073	−0.344, 0.210
BMI (kg/m^2)	0.181	−0.110, 0.445	−0.079	−0.350, 0.204	0.140	−0.153, 0.409	−0.236	−0.483, 0.045
Hypertension	0.264	−0.024, 0.512	−0.123	−0.388, 0.160	0.217	−0.074, 0.474	−0.200	−0.453, 0.083
Diabetes	0.111	−0.181, 0.389	0.022	−0.258, 0.298	0.121	−0.171, 0.394	−0.212	−0.463, 0.071
Hyperlipidemia	0.166	−0.126, 0.432	**−0.308**	−0.540, −0.033	0.181	−0.111, 0.444	**−0.365**	−0.584, -0.096
Current smoker	0.085	−0.206, 0.362	**−0.295**	−0.530, −0.018	0.134	−0.158, 0.405	−0.119	−0.384, 0.165
Family history	−0.165	−0.431, 0.127	0.011	−0.268, 0.288	−0.136	−0.407, 0.156	−0.042	−0.316, 0.239
Heart rate (bpm)	**0.394**	0.121, 0.611	−0.042	−0.316, 0.239	0.083	−0.208, 0.361	0.086	−0.197, 0.356
CACS	**0.438**	0.153, 0.655	**−0.340**	−0.576, −0.052	**0.428**	0.169, 0.664	−0.085	−0.372, 0.218
CAD-RADS	**0.423**	0.156, 0.633	**−0.392**	−0.605, −0.128	**0.526**	0.282, 0.706	−0.236	−0.482, 0.046
Total coronary calcium volume (mm^3)	**0.486**	0.226, 0.681	**−0.512**	−0.695, −0.267	**0.492**	0.234, 0.686	−0.161	−0.426, 0.129
Total coronary plaque volume (mm^3)	**0.388**	0.108, 0.611	**−0.469**	−0.665, −0.213	**0.373**	0.091, 0.600	−0.084	−0.359, 0.205

Pearson's correlation unless otherwise noted. *Spearman's correlation. Statistically significant correlations with P values < 0.05 are listed in bold.
EID: Energy-integrating detector. PCD: Photon-counting detector. Bv: body/vascular kernel. EAT: Epicardial adipose tissue. BMI: Body mass index. CI: Confidence interval. bpm: Beats per minute. CACS: Coronary artery calcium scoring. CAD-RADS: Coronary artery disease reporting and data system.

Table A.2 and Table A.3. In both comparisons, increased EAT volume and lower EAT attenuation coincided with increased CACS, CAD-RADS scores, and total coronary calcium and plaque volume.

4. Discussion

By comparing prospectively acquired data of EAT volume and attenuation measurements between an EID- and a PCD-CT system in the same patients, we found that down-sampling of UHR data acquired on a PCD-CT system does not produce the same results as EID-CT acquisitions when slice thickness and kernel are matched. The most closely matching EAT volumes were achieved between the 0.6 mm slice thickness EID and 0.2 mm slice thickness PCD-UHR$_{Bv48}$ reconstructions, while PCD-UHR$_{Bv40}$ and PCD-UHR$_{Bv48}$ matched closest to the EID-CT regarding attenuation.

Increased EAT volumes and lower EAT attenuations have been linked to increased coronary calcium, elevated inflammatory serum markers, and increased risks of MACE, potentially providing incremental value as prognostic markers [2,11–13]. In our data, moderate correlations were observed between EAT volume and attenuation and markers of cardiovascular disease such as CACS, CAD-RADS score, total coronary calcium volume, and total coronary plaque volume, all of which have been described as independent predictors of MACE [13]. Interestingly, there was a lack of correlation between EAT volume and body mass index. EAT is thought to be a biologically active organ that interacts with the heart due to a shared microcirculation and lack of separating fascia. On a molecular level, it has been shown that different genes are active in EAT compared to subcutaneous adipose tissue, potentially explaining the lack of correlation [14].

Aspects such as higher spatial resolution, less calcium blooming, and "always on" spectral imaging of PCD-CTs have already demonstrated significant differences regarding luminal stenosis quantification and potential for fewer referrals for follow-up invasive coronary angiography compared to EID-CTs [15,16]. Our study design utilized a unique patient cohort, who underwent EID and PCD CCTA within a maximum of 30 days of each other, allowing an opportunity to analyze fundamental differences in detector technology on an intra-individual basis. While absolute EAT volume and attenuation differed between the EID- and the PCD-CT systems, the tendencies of lower attenuation and larger volumes correlated with cardiovascular risk factors for MACE on both detectors, in line with other studies [10,13,17].

4.1. Differences in EAT measurements between EID-CT and PCD-CT

4.1.1. Slice thickness and kernel selection

Thicker slice reconstructions reduce spatial resolution, leading to increased partial volume effects, a phenomenon where multiple adjacent tissues contribute to the density of a voxel [18]. Softer reconstruction kernels smooth CT images through spatial interpolation which also reduces image resolution and like thicker slices lead to an increased partial volume effect [18]. Both the increase of slice thickness or the decrease in kernel sharpness lead to a reduction in noise and to an averaging of voxel densities towards the mean [19]. These effects were reflected in our patient cohort, where attenuation histograms narrowed in the PCD-DS reconstructions and widened as thinner slices and sharper kernels were applied. PCD-UHR$_{Bv48}$ reconstructions demonstrated attenuation histograms most similar to the EID-CT (Fig. 3F), consequently correlating best with the EID reconstruction for volume and relatively good regarding attenuation. Unfortunately, higher sharpness kernels suffered from increased noise resulting in pixels outside the threshold being counted as EAT and potentially contributing to the broader difference in EAT volume and attenuation when comparing PCD-UHR$_{Bv64}$ to EID reconstructions. Overall, PCD-UHR$_{Bv48}$ reconstructions came closest to EID findings.

4.1.2. Fundamental detector differences: Polychromatic vs T3D

Polychromatic EID-CT acquisitions use the broad spectrum of energy levels to produce a single image, with higher level photons weighted more than lower energy ones. In a PCD-CT, photons can be separated based on their energies and thresholds can be applied to filter out certain energy levels, e.g. low energy thresholds at 20–30 keV to filter out electronic noise [20]. The missing low energy signal on PCD-CT may have contributed to minor differences in EAT measurements.

4.1.3. Differences between Advanced Modeled iterative reconstruction and Quantum iterative reconstruction

Both ADMIRE and QIR are propriety iterative reconstruction algorithms used to help improve image quality by reducing noise and artefacts, and lower required radiation doses [21,22]. Bache and Samei have shown that QIR on PCD-CT better preserves noise textures than ADMIRE on EID-CTs (7 % vs 20 % shift in noise texture going from iterative reconstruction "off" to "maximum") [23]. They recommend an increase of kernel sharpness by one step and iterative reconstruction by 1–2 steps on PCD-CTs when matching noise profiles to EID-CTs, corresponding to our observations on EAT volume and attenuation.

4.2. Limitations

Our study possesses a few limitations. Due to the clinical indications of the CCTAs, all datasets were acquired after the injection of contrast. Furthermore, acquisition of UHR data concurrent with spectral information for the reconstruction of virtual non-contrast images was not possible with the available PCD scanner software at the time of analysis. We did not assess changes in EAT volume or attenuation regarding different iterative reconstruction levels.

5. Conclusion

EAT attenuation and volume measurements demonstrated different absolute values between PCD-UHR, PCD-DS, and EID-CT reconstructions on an intra-individual level. Although, similar tendencies were observed, new protocols and threshold ranges need to be developed to allow comparison between PCD-CT and EID-CT data.

Funding

This research was partially funded by a grant from Siemens Healthineers.

CRediT authorship contribution statement

Dmitrij Kravchenko: Data curation, Formal analysis, Investigation, Methodology, Visualization, Writing – original draft, Writing – review & editing. **Milan Vecsey-Nagy:** Data curation, Supervision, Writing – review & editing. **Giuseppe Tremamunno:** Data curation, Writing – review & editing. **U. Joseph Schoepf:** Funding acquisition, Resources. **Jim O'Doherty:** Resources, Validation, Writing – review & editing. **Julian A. Luetkens:** Writing – review & editing. **Daniel Kuetting:** Writing – review & editing. **Alexander Isaak:** Writing – review & editing. **Muhammad Taha Hagar:** Investigation, Writing – review & editing. **Tilman Emrich:** Conceptualization, Investigation, Methodology, Project administration, Supervision, Validation, Writing – review & editing. **Akos Varga-Szemes:** Conceptualization, Funding acquisition, Methodology, Project administration, Resources, Supervision, Visualization, Writing – review & editing.

Declaration of competing interest

The authors declare the following financial interests/personal relationships which may be considered as potential competing interests: UJS receives institutional research support and / or personal fees from Bayer, Bracco, Elucid Bioimaging, Guerbet, HeartFlow, Keya Medical, and Siemens. AVS receives institutional research support and / or personal fees from Elucid Bioimaging and Siemens. TE received a speaker fee and travel support from Siemens, institutional research support by Siemens and is a consultant at Circle CVI. JOD is an employee of Siemens.

Acknowledgements

None.

Ethics approval

This study was performed in line with the principles of the Declaration of Helsinki. Approval was granted by the local Institutional Review Board.

Consent to participate

Informed consent was obtained from all individual participants included in the study.

Consent to publish

The authors affirm that human research participants provided informed consent for publication of the images in this manuscript.

Data statement

All available data will be provided upon reasonable request.

Appendix A. Supplementary data

Supplementary data to this article can be found online at https://doi.org/10.1016/j.ejrad.2024.111728.

References

[1] T.H. Le Jemtel, R. Samson, K. Ayinapudi, et al., Epicardial Adipose Tissue and Cardiovascular Disease, Curr. Hypertens. Rep. 21 (5) (2019).
[2] M. Goeller, S. Achenbach, M. Marwan, et al., Epicardial adipose tissue density and volume are related to subclinical atherosclerosis, inflammation and major adverse cardiac events in asymptomatic subjects, J. Cardiovasc. Comput. Tomogr. 12 (1) (2018) 67.
[3] T. Mazurek, L.F. Zhang, A. Zalewski, et al., Human epicardial adipose tissue is a source of inflammatory mediators, Circulation 108 (20) (2003) 2460–2466.
[4] J. Narula, Y. Chandrashekhar, A. Ahmadi, et al., SCCT 2021 Expert Consensus Document on Coronary Computed Tomographic Angiography: A Report of the Society of Cardiovascular Computed Tomography, J. Cardiovasc. Comput. Tomogr. 15 (3) (2021).
[5] J. Knuuti, W. Wijns, A. Saraste, et al., 2019 ESC Guidelines for the diagnosis and management of chronic coronary syndromes: The Task Force for the diagnosis and management of chronic coronary syndromes of the European Society of Cardiology (ESC), European Heart Journal 41(3) (2020/01/14).
[6] M.J. Willemink, M. Persson, A. Pourmorteza, et al., Photon-counting CT: Technical principles and clinical prospects, Radiology 289 (2) (2018) 293–312.
[7] S. Baba, H.A. Jacene, J.M. Engles, et al., CT Hounsfield Units of Brown Adipose Tissue Increase with Activation: Preclinical and Clinical Studies, J. Nucl. Med. 51 (2) (2010) 246–250.
[8] K.J. Rosenquist, J.M. Massaro, A. Pedley, et al., Fat Quality and Incident Cardiovascular Disease, All-Cause Mortality, and Cancer Mortality, J. Clin. Endocrinol. Metab. 100 (1) (2015) 227–234.
[9] M. Marwan, S. Koenig, K. Schreiber, et al., Quantification of epicardial adipose tissue by cardiac CT: Influence of acquisition parameters and contrast enhancement, Eur. J. Radiol. 121 (2019) 108732.
[10] N.N. Pandey, S. Sharma, P. Jagia, et al., Epicardial fat attenuation, not volume, predicts obstructive coronary artery disease and high risk plaque features in patients with atypical chest pain, Br. J. Radiol. 93 (1114) (2020).
[11] B.T. Franssens, H.M. Nathoe, F.L.J. Visseren, et al., Relation of Epicardial Adipose Tissue Radiodensity to Coronary Artery Calcium on Cardiac Computed Tomography in Patients at High Risk for Cardiovascular Disease, Am. J. Cardiol. 119 (9) (2017) 1359–1365.
[12] V. Brandt, J. Decker, U.J. Schoepf, et al., Additive value of epicardial adipose tissue quantification to coronary CT angiography–derived plaque characterization and CT fractional flow reserve for the prediction of lesion-specific ischemia, Eur. Radiol. 32 (6) (2022) 4243–4252.
[13] B. Chong, J. Jayabaskaran, J. Ruban, et al., Epicardial Adipose Tissue Assessed by Computed Tomography and Echocardiography Are Associated with Adverse Cardiovascular Outcomes: A Systematic Review and Meta-Analysis, Circulation: Cardiovascular Imaging 16(5) (2023) E015159-E015159.
[14] E.A. McAninch, T.L. Fonseca, R. Poggioli, et al., Epicardial adipose tissue has a unique transcriptome modified in severe coronary artery disease, Obesity (Silver Spring Md.) 23 (6) (2015) 1267–1278.
[15] M.C. Halfmann, S. Bockius, T. Emrich, et al., Ultrahigh-Spatial-Resolution Photon-counting Detector CT Angiography of Coronary Artery Disease for Stenosis Assessment, Radiology 310 (2) (2024.).
[16] J. Simon, Á. Hrenkó, N.M. Kerkovits, et al., Photon-counting detector CT reduces the rate of referrals to invasive coronary angiography as compared to CT with whole heart coverage energy-integrating detector, J. Cardiovasc. Comput. Tomogr. 18 (1) (2024.).
[17] Z. Gao, Y. Zuo, L. Jia, et al., Association between epicardial adipose tissue density and characteristics of coronary plaques assessed by coronary computed tomographic angiography, Int. J. Cardiovasc. Imaging 38 (3) (2022) 673–681.

[18] S. Achenbach, K. Boehmer, T. Pflederer, et al., Influence of slice thickness and reconstruction kernel on the computed tomographic attenuation of coronary atherosclerotic plaque, J. Cardiovasc. Comput. Tomogr. 4 (2) (2010) 110–115.
[19] D.S. Gierada, A.J. Bierhals, C.K. Choong, et al., Effects of CT Section Thickness and Reconstruction Kernel on Emphysema Quantification: Relationship to the Magnitude of the CT Emphysema Index, Acad. Radiol. 17 (2) (2010) 146.
[20] S. Leng, G.V. Toia, S. Hoodeshenas, et al., Standardizing technical parameters and terms for abdominopelvic photon-counting CT: laying the groundwork for innovation and evidence sharing, Abdominal Radiology 2024 (2024-05-20).
[21] T. Sartoretti, A. Landsmann, D. Nakhostin, et al., Quantum Iterative Reconstruction for Abdominal Photon-counting Detector CT Improves Image Quality, Radiology 303(2) (2022-02-01).
[22] M.J. Willemink, P.A. de Jong, T. Leiner, et al., Iterative reconstruction techniques for computed tomography Part 1: Technical principles, Eur. Radiol. 2013 23:6 23 (6) (2013-01-12).
[23] S.T. Bache, E. Samei, A methodology for incorporating a photon-counting CT system into routine clinical use, J. Appl. Clin. Med. Phys. 24 (8) (2023/08).